metals

MDPI

Article

Understanding the Recovery of Rare-Earth Elements by Ammonium Salts

Jamie P. Hunter [1], Sara Dolezalova [1], Bryne T. Ngwenya [2], Carole A. Morrison [1] and Jason B. Love [1,*]

[1] EaStCHEM School of Chemistry, University of Edinburgh, Edinburgh EH9 3FJ, UK; Jamie.P.Hunter@ed.ac.uk (J.P.H.); s1304479@sms.ed.ac.uk (S.D.); carole.morrison@ed.ac.uk (C.A.M.)

[2] School of Geosciences, University of Edinburgh, Edinburgh EH9 3FE, UK; Bryne.Ngwenya@ed.ac.uk

* Correspondence: jason.love@ed.ac.uk; Tel.: +44-131-650-4762

Received: 4 June 2018; Accepted: 15 June 2018; Published: 19 June 2018

Abstract: While the recovery of rare earth elements (REEs) from aqueous solution by ionic liquids (ILs) has been well documented, the metal compounds that are formed in the organic phase remain poorly characterized. Using spectroscopic, analytical, and computational techniques, we provide detailed chemical analysis of the compounds formed in the organic phase during the solvent extraction of REEs by [(n-octyl)$_3$NMe][NO$_3$] (**IL**). These experiments show that REE recovery using **IL** is a rapid process and that **IL** is highly durable. Karl-Fischer measurements signify that the mode of action is unlikely to be micellar, while ions of the general formula REE(NO$_3$)$_4$(**IL**)$_2^-$ are seen by negative ion electrospray ionization mass spectrometry. Additionally, variable temperature ^{139}La nuclear magnetic resonance spectroscopy suggests the presence of multiple, low symmetry nitrato species. Classical molecular dynamics simulations show aggregation of multiple **IL**s around a microhydrated La^{3+} cation with four nitrates completing the inner coordination sphere. This increased understanding is now being exploited to develop stronger and more selective, functionalized ILs for REE recovery.

Keywords: ionic liquids; extraction; rare-earths; mass-spectrometry; computational modelling

1. Introduction

Ionic liquids (ILs) are particularly desirable as reagents and solvents due to their ability to be tailored through the modification of their cation and anion components, and their perception as having "green credentials" due to their negligible vapor pressure, high thermal stability, and non-flammability [1]. They are often immiscible with aqueous phases, and this feature, combined with their other properties, has been exploited in the separation and recovery of metals such as the rare earth elements (REEs) by solvent extraction [2–8]. The use of ILs in solvent extraction processes can minimize extractant loss, reduce environmental contamination, and limit the use of volatile organics as diluents [3,9]. This contrasts with the purification of REEs in China by traditional solvent extraction techniques, which have been found to produce 20 million tons of wastewater contaminated with, in some cases, an excess of 50 g/L of organic compounds [10]. ILs are therefore not only research curiosities, but also have strategic industrial importance.

The transport of REEs from aqueous (acidic) solutions into an immiscible IL phase has been extensively studied for a variety of hydrophobic ILs, and some, but not always complementary, insight into the mechanisms of extraction has been gained [2]. The transport of Nd or Eu in a biphasic aqueous/C$_4$mim$^+$Tf$_2$N$^-$ IL system (C$_4$mim = *N*-methyl-*N*-butylimidazolium; NTf$_2^-$ = bis(triflimide) anion $^-$N{SO$_2$CF$_3$}$_2$) by the acetylacetonate 2-thenoyltrifluoroacetone (tta) has been shown by Extended X-ray Absorption Fine Structure (EXAFS) spectroscopy, molecular dynamics (MD) simulations, and fluorescence lifetime measurements to proceed through the formation of

the ion pair $[C_4mim][Ln(tta)(Tf_2N)]$ [11]. Further studies have shown that the water molecules in the hydrate $[Eu(tta)_3(OH_2)_3]$ are substituted by the Tf_2N^- anion, with the $[Ln(tta)(Tf_2N)]^-$ anion identified in the ESI-MS of the IL phase [12]. ILs of hydrophobic ammonium (R_4N^+, where R is an alkyl chain) and phosphonium (R_4P^+) cations with a variety of coordinating anions have been studied; anions of the phosphorus acids tend to favor recovery of the heavy REEs, whereas the use of more simple anions such as nitrate or Tf_2N^- favors light REE recovery. For example, the alkyl ammonium chloride Aliquat® 336 (A336, MeR_3NCl, where R = 2:1 C_8:C_{10} alkyl chains of various isomers [13]) when used in combination with the anion of the dialkylphosphoric acid, D2EHPA, $((RO)_2P{=}O(OH)$, R = ^{t}BuCH$_2$(CH$_3$)CHCH$_2$) or the phosphinic acid Cyanex® 272 ($R_2P(O)(OH)$, R = ^{t}BuCH$_2$(CH$_3$)CHCH$_2$) produces bifunctional ionic liquid extractants (Bif-ILs) which recover Nd and Pr from aqueous acidic chloride [14]; slope analyses suggest a 3:1 Bif-IL:Ln stoichiometry in the transported species, possibly $LnCl_3(Bif\text{-}IL)_3$. Similar A336/dialkylphosphate or diglycolamate Bif-ILs recovered europium from acidic nitrate solutions and slope analysis suggested a 3:1 Bif-IL:Ln stoichiometry consistent with $Eu(NO_3)_3(Bif\text{-}IL)_3$ [15]. In contrast, combinations of A336 and the trialkylphosphonate, DEHEHP, $((RO)_2(R)P{=}O$, R = 2-ethylhexyl) have been found to recover REEs from acidic nitrate under high nitrate salt conditions, in this case by the formation of either $Ln(NO_3)_3(DEHEHP)_x$ or the ion pairs $[A336]_{n\text{-}3}[Ln(NO_3)_n]$ as suggested by slope analysis and infrared (IR) spectroscopy [3]. Furthermore, a Bif-IL comprising $PR_3R'^+$ cations (R = hexyl, R′ = tetradecyl) and Cyanex® 272 anions extracts the heavy REEs preferentially, but in this case slope analysis and release of acid on REE transport suggests the formation of $Ln(O_2PR_2)_3$ complexes through a cation-exchange mechanism [16].

While [A336]Cl does not extract REEs from aqueous solution, it is well known that $[A336]NO_3$ is effective for light REE recovery, particularly under high aqueous nitrate concentrations (through salting-out [17]) [18,19]. This effect has been exploited in REE separation using $[A336]NO_3$ and EDTA (ethylenediamine tetraacetic acid) to partition the light and heavy REEs in the IL and the aqueous phase, respectively [20]. Initial interpretations of the mechanism of transport by $[A336]NO_3$ suggest the formation of ion pairs $[A336]_{n\text{-}3}[Ln(NO_3)_n]$ or alternatively IL adducts of neutral Ln complexes, i.e., $Ln(NO_3)_3\{[A336]NO_3\}_3$. Further studies have proposed, through slope analysis, the formation of simple lanthanide nitrate anions $[A336]Ln(NO_3)_4$ or those with more complex speciation $[A336]Ln(NO_3)_4\{Ln(NO_3)_3\}$ [21]. The discrete ion pairs $[A336]_2[Ln(NO_3)_5]$ and $[A336]_3[Ln(NO_3)_6]$ may also be observed, as suggested by Nuclear Magnetic Resonance (NMR) [22,23], IR [24], and UV-vis spectroscopic analysis [22], and X-ray crystallography (see, for example, [25–27]). The relevant hexakis(nitrato) lanthanide ion $Nd(NO_3)_6^{3-}$ has been characterized by EXAFS in *dry* $[C_4mim][Tf_2N]$ and shows high stability constants by optical spectroscopy [28], whereas in *wet* $[C_4mim][Tf_2N]$ ElectroSpray Ionization Mass Spectrometry (ESI-MS) analysis suggests the formation of $Eu(NO_3)_4^-$ anions [29]. ILs comprising $[PR_3R']$ cations (R = hexyl, R′ = tetradecyl) and nitrate anions have also been exploited in the separation of REEs from Co and Ni by solvent extraction, with slope analysis suggesting the formation of the ion pairs $[PR_3R']_2Sm(NO_3)_5$ and $[PR_3R']_3La(NO_3)_6$ in the IL phase [30].

While it is clear that hydrophobic ILs and Bif-ILs are effective in the extraction and separation of REEs, with or without added organic diluent, the species formed in the hydrophobic phase are diverse and poorly characterized, which impacts the chemical understanding of the separation process. The formation of ion pairs of various stoichiometries is prevalent, yet seemingly counterintuitive, as we have shown computationally that nitrate anions are more likely to be bound in the outer-sphere of a hydrated Ln^{3+} cation, e.g., $[Ln(OH_2)_6][NO_3]_3$ [31]; this is supported by the lack of extraction of Ln nitrates by common anion exchangers that have been exploited extensively for the recovery of halometalates of transition metals [32–34]. Herein, we review the recovery of REEs by the simple analogue of $[A336]NO_3$, $[(^n\text{octyl})_3NMe]NO_3$ (**IL**) under high $NaNO_3$ conditions and provide characterization of the extracted species by ^{139}La NMR spectroscopy, ESI-MS, and computational modelling in order to understand better the mode of action of these reagents.

2. Materials and Methods

2.1. Materials

Unless otherwise stated, all solvents and reagents were purchased from Sigma-Aldrich (Gillingham, UK), Fisher scientific UK (Loughborough, UK), Alfa Aesar (Heysham, UK), Acros Organics (Geel, Belgium), or VWR international (Lutterworth, UK) and used without further purification. Deionised water was produced using a Milli-Q purification system (Sigma-Aldrich, Gillingham, UK).

2.2. Characterisation and Computational Techniques

NMR spectra were recorded at 298K on a Bruker AVA400, AVA500 or AVA600 spectrometer (Coventry, UK) operating at 399.90, 500.12, or 599.95 MHz, respectively, for ^{1}H, and 100.55, 125.76, or 150.83 MHz, respectively, for ^{13}C. ESI-MS measurements were recorded in negative-ion mode using the standard Bruker ESI sprayer operated in "infusion" mode coupled to a Bruker SolariX Fourier transform ion cyclotron resonance mass spectrometer (Bruker Daltronics, Coventry, UK). Direct infusion spectra were a sum of 10 acquisitions. All mass spectra were analyzed using DataAnalysis software version 4.1 SR1 build 359 (Bruker Daltronics, Coventry, UK) and ions were assigned manually. A Perkin Elmer Optima 8300 Inductively Coupled Plasma Optical Emission Spectrometer (ICP-OES) (Beaconsfield, UK) was used to determine metal concentration (in 1-methoxy-2-propanol). Samples were taken up by a peristaltic pump at a rate of 1.0 mL·min^{-1} into a Gem Tip cross flow nebulizer and glass cyclonic spray chamber. Conditions for plasma, auxiliary, and nebulizer argon gas flows were 18, 1.5, and 0.5 L·min^{-1} with 1500 W RF forward power, respectively. ICP-OES external calibration standards were obtained from VWR International or Sigma-Aldrich. Karl-Fischer titrations were carried out using a Mettler-Toledo Coulometric KF Titrator C30S with DM 143-SC probe (Leicester, UK), and pH measurements were obtained using a Mettler Toledo Excellence Titrator T5 with a DGi115-SC probe (Leicester, UK). Nitrate anion concentrations were determined using an ICS-110 RFIC ion chromatography system with AS22 diluent. Infrared spectrum were acquired using a Nicolet Avatar 360 FT-IR spectrometer (Fisher Scientific, Loughborough, UK).

Classical molecular dynamics (MD) simulations were employed using the Optimized Potentials for Liquid Simulations—All Atoms (OPLS-AA) force field within the Large Scale Atomic/Molecular Parallel Simulations (LAMMPS) software package from Sandia National laboratories, Albuquerque, NM, USA [35]. An initial model, comprising three **IL**s, three NO_3^-, three H_2O, and one La^{3+} randomly distributed in a cubic simulation cell of length 60 Å was constructed using Packmol [36]. The generated xyz file was then converted into a LAMMPS data file using the Visual Molecular Dynamics (VMD) Topo tools [37]. The optimized geometries for the ammonium cation (octyl)$_3$NMe$^+$, NO_3^-, toluene, and water were obtained using the Gaussian 09 program (Gaussian Inc., Wallingford, UK) and with the B3LYP/6-31G** level of theory applied to all atoms present [38]. Structures were considered optimized when the forces and atomic displacements fell to within the program default convergence criteria. The integration time step of the MD simulations was set to 0.5 fs, and time increments accrued using the standard Velocity-Verlet algorithm. In total, system dynamics were accrued for a minimum of 10,200 ps. This included 500 ps equilibration time under canonical (constant Number of atoms, Volume, and Temperature, NVT) ensemble conditions followed by a production run of 9700 ps under isothermal-isobaric conditions (constant number of atoms, pressure, and temperature, NPT). NVT and NPT conditions were themostated at room temperature and pressure using the Nosé–Hoover thermostat-barostat system [39,40].

*2.3. Synthesis of Trioctylmethylammonium Nitrate (**IL**)*

Following a standard preparation [41], iodomethane (4.44 g, 31 mmol) was added dropwise to a stirred solution of trioctylamine (8.85 g, 25 mmol) in THF (100 mL), and the mixture was stirred at

40 °C for 12 h under a flow of N_2. The crude mixture was concentrated under vacuum, diluted with diethyl ether (100 mL), and contacted three times with an aqueous solution of sodium nitrate (7 M) (1 h, room temperature). The organic phase was separated and concentrated under vacuum to yield a viscous orange oil (100%). ^{1}H NMR (500 MHz, $CDCl_3$): δ_H 3.41–3.35 (m, 6H, NC**H**$_2$), 3.24 (s, 3H, NC**H**$_3$), 1.74–1.64 (m, 6H, C**H**$_2$), 1.43–1.23 (m, 30H, C**H**$_2$), 0.89 (t, J = 6.8 Hz, 9H, CH_2C**H**$_3$). ^{13}C{^{1}H} NMR (126 MHz, $CDCl_3$): δ_C 61.70, 48.83, 31.62, 29.10, 29.01, 26.30, 22.57, 22.43, 14.04.

2.4. General REE Recovery Procedure

An aqueous solution of the hydrated REE nitrate $Ln(OH_2)_n(NO_3)_3$ (La, Nd, or Dy, 0.01 M unless otherwise stated) (2 mL) was contacted with a toluene organic phase containing tri-n-octylmethyl ammonium nitrate **IL** (0.10 M unless otherwise stated) (2 mL) and stirred (12 h, 1000 rpm, 25 °C). The phases were then separated physically and diluted (80×) with 1-methoxy-2-propanol for ICP-OES analysis. La, Nd, and Dy were chosen as light, intermediate, and heavy REEs.

3. Results and Discussion

*3.1. Solvent Extraction of La, Nd, and Dy by **IL***

A series of REE recovery experiments were carried out in which the concentrations of the **IL**, $NaNO_3$ salt, and HNO_3, and extraction time were varied (see Table S1 for data in terms of distribution coefficients). Additionally, the ability to back-extract the metal from the organic phase into a fresh aqueous phase, in conjunction with recyclability of **IL** was studied. The **IL** in toluene solution (0.01–1.00 M) is found to transport La, Nd, and Dy (0.01 M) from aqueous $NaNO_3$ (7 M) into the organic phase in the order La > Nd > Dy (Figure 1). This trend was observed in all further studies, is similar to that seen previously for this class of extractants, and contrasts the typical commercial reagents for REE recovery, including naphthenic acid and the dialkylphosphoric acid D2EHPA that display the reverse preference [42–46]. Maximum recoveries of La (100%), Nd (98%), and Dy (92%) were obtained at 1.00 M **IL** with an expected gradual decrease in percentage recovery observed as the concentration of **IL** (M) decreased [14,15].

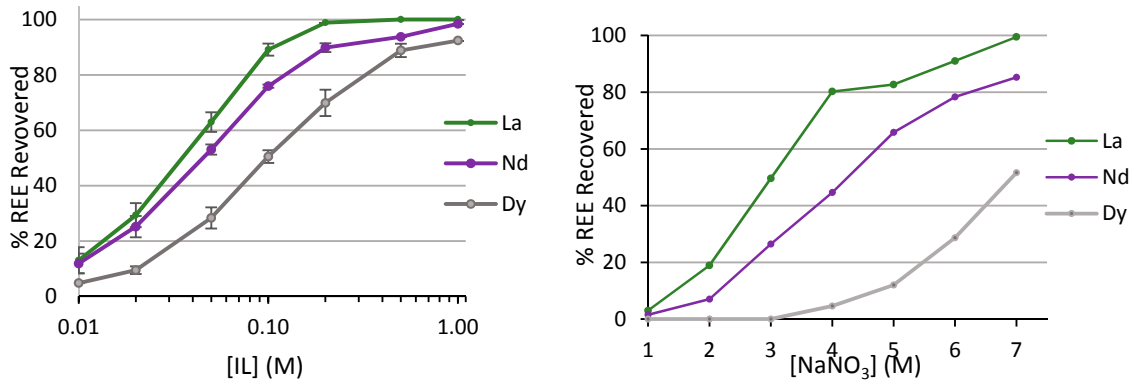

Figure 1. (**Left**): the recovery of La, Nd, and Dy (0.01 M) from an $NaNO_3$ (7 M) aqueous solution varying **IL** concentration (0.01–1.0 M) in toluene (recorded in triplicate). (**Right**): The recovery of La, Nd, and Dy (0.01 M) using **IL** (0.10 M) in toluene varying $NaNO_3$ concentration (1–7 M). Interpolation used to aid the eye only.

When **IL** concentration was constant (0.1 M) and $NaNO_3$ salt varied (1–7 M), the REE transportation into the organic phase increased substantially as $NaNO_3$ salt concentration increased (Figure 1), in line with previous work [3,4]. For La, Nd, and Dy minimal recovery (<5%) was obtained at 1 M $NaNO_3$, whereas at 7 M $NaNO_3$, 99% La, 85% Nd, and 52% Dy were recovered. Slope analysis

(Figure S1) provided a relationship of 1:3 between La or Nd and $NaNO_3$, in accordance with previous work [3], while a relationship of 1:1.5 was observed between La or Nd and **IL**.

A substantial reduction in the transport of La, Nd, and Dy (0.01 M) from the aqueous phase with **IL** (0.10 M) is seen as the concentration of HNO_3 is increased (0.005–1.00 M) (Figure 2), with a pronounced decrease seen starting at 0.1 M HNO_3 and minimal recovery (<5%) of all REEs at 1.0 M HNO_3. The mixed chain/isomer analogue of **IL**, $[A336]NO_3$ is known to transport HNO_3 from the aqueous phase [21], so it is likely that competition between REE recovery and acid extraction occurs at higher concentrations of HNO_3 (see below).

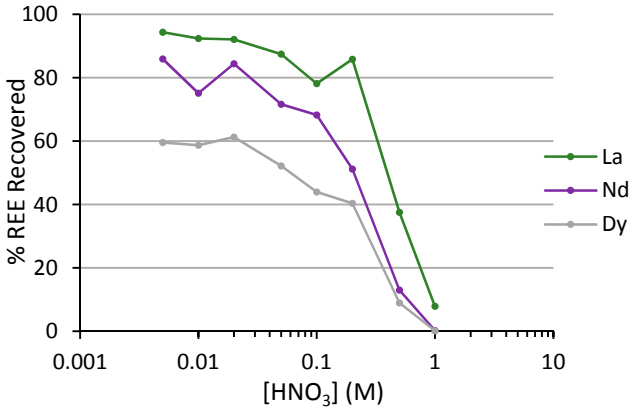

Figure 2. The extraction of La, Nd and Dy (0.01 M) in using **IL** (0.1 M) with varying HNO_3 (0.005–1.0 M) at constant NO_3^- concentration (7 M). Interpolation used to aid the eye only.

Using the optimized conditions of 0.01 M **IL** and 7 M $NaNO_3$, it was found that the transport of La from the aqueous to the organic phase by **IL** is rapid (Figure 3), as seen in similar studies [3,47,48]; after only 60 s the concentration of La in the organic phase is maximized.

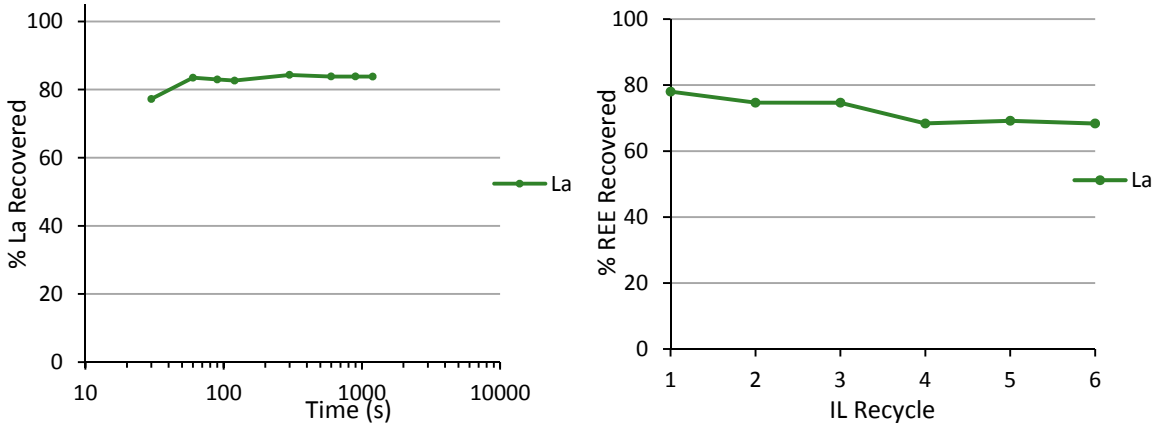

Figure 3. (**Left**): The recovery of La (0.01 M) in $NaNO_3$ (7 M) using **IL** (0.1 M) with varying time (seconds). (**Right**): The recycling of IL (0.1 M) to load La (0.01 M) from aqueous $NaNO_3$ (7 M) following multiple load/strip cycles. Water was used to strip La (100%). Interpolation used to aid the eye only.

The back-extraction of the REEs from the **IL** organic phase into a fresh aqueous solution was studied and shows that complete back-extraction is achieved using water (Figure S2) [3,4,47], in contrast to pH swing reagents such as D2EHPA that typically require acidic strip conditions [42,43,49,50]. Some selectivity in the back-extraction process is achieved through the addition of $NaNO_3$ to the aqueous phase. While Dy, the heavier REE, is readily back-extracted (>95%) by aqueous $NaNO_3$ (<5 M), the transport of La, the lighter REE into the aqueous phase is hindered under these conditions,

with <20% stripped. Additionally, **IL** is durable and readily reusable, with only a minimal performance decrease (5%) seen following six load and strip cycles (Figure 3), with the loss observed likely due to entrainment [47].

*3.2. Evaluation of the Mechanism of Ln Recovery by **IL***

3.2.1. Karl-Fischer Analysis of Water Content

Some metal recovery processes, in particular those involving solvating reagents, operate by a reverse micelle mechanism. Here, the metal ion is solvated (and hydrated) by a water pool, which is stabilized in the organic phase by spontaneous assembly of the hydrophobic extractant molecules to form micellar aggregates [51–56]. A feature of reverse-micelle mechanisms is therefore the transport of water into the organic phase, with increasing amounts associated with increasing metal extraction. The water content of the organic phase containing **IL** (0.01–1.00 M) was measured by Karl-Fischer titration following various aqueous phase contacts (Figure 4). These included extraction of La, Nd, and Dy (0.01 M) from $NaNO_3$ (7 M), contact with aqueous $NaNO_3$ (7 M), and contact with pure water. It is seen that **IL** is naturally hydrophilic, solubilizing a proportional amount of water in relation to its concentration. FT-IR studies have shown that ILs of ammonium cations readily extract water, indicated by the presence of a strong broad stretch at ~3450 cm^{-1} following contact with water [3,4,47,57]. The water content seen for the metal-loaded **IL** phase is comparable, albeit slightly lower than that seen for the water-only contact, indicating that rare-earth extraction is not dependent on the extraction of water and that a reverse-micelle mechanism of extraction is unlikely. Interestingly, when the concentration of **IL** is constant but the concentration REE is varied, a decrease in extracted water is observed, and may be due to the **IL** preferentially interacting with the REE and displacing water into the aqueous phase.

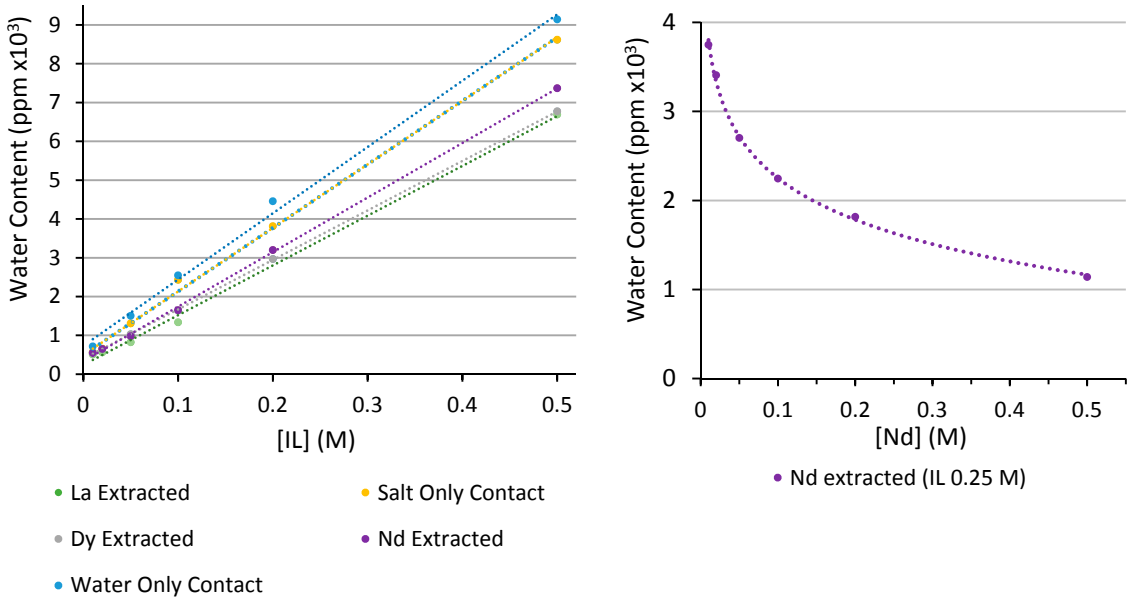

Figure 4. (**Left**): the water content (ppm) of **IL** (0.01–1.00 M) organic phases determined by Karl-Fischer titration. (**Right**): the water content (ppm) of organic phase **IL** (0.25 M) with varying Nd (0.01–0.5 M) was also determined by Karl-Fischer titration. Interpolation used to aid the eye only.

3.2.2. Nitric Acid and Nitrate Transport by **IL**

The **IL** (0.10 M) in toluene was contacted with aqueous phases of varying HNO_3 concentration (0.01–1.00 M) containing $NaNO_3$ (0 and 5 M) (5 min). The organic phase was then contacted with water (5 min) and the pH of the aqueous phase measured. As the HNO_3 concentration of the initial

aqueous phase increases, the pH of the final aqueous phase decreases, indicative of an increasing amount of HNO_3 being extracted by **IL** (Figure 5). The pH of the aqueous strip phase when the initial acidic solution was in 5 M $NaNO_3$ is lower in each instance when compared with the absence of $NaNO_3$, consistent with a salting-out effect. The amount of NO_3^- anions in the final aqueous strip from 5 M $NaNO_3$ was determined by Na analysis using ICP-OES (Figure 5) and ion-chromatography (IC) (Figure 5) and shows that when $NaNO_3$ is present, the additional NO_3^- extracted is derived predominately from the extraction of HNO_3; Na is not transported as the quantity of Na cations is independent of HNO_3 concentration. The IC data indicate that the concentration of NO_3^- anions in the final aqueous phase increases as HNO_3 increases. Collectively, these data show that the transport of NO_3^- anions into the organic phase by IL is due to co-extraction of H^+ rather than Na^+.

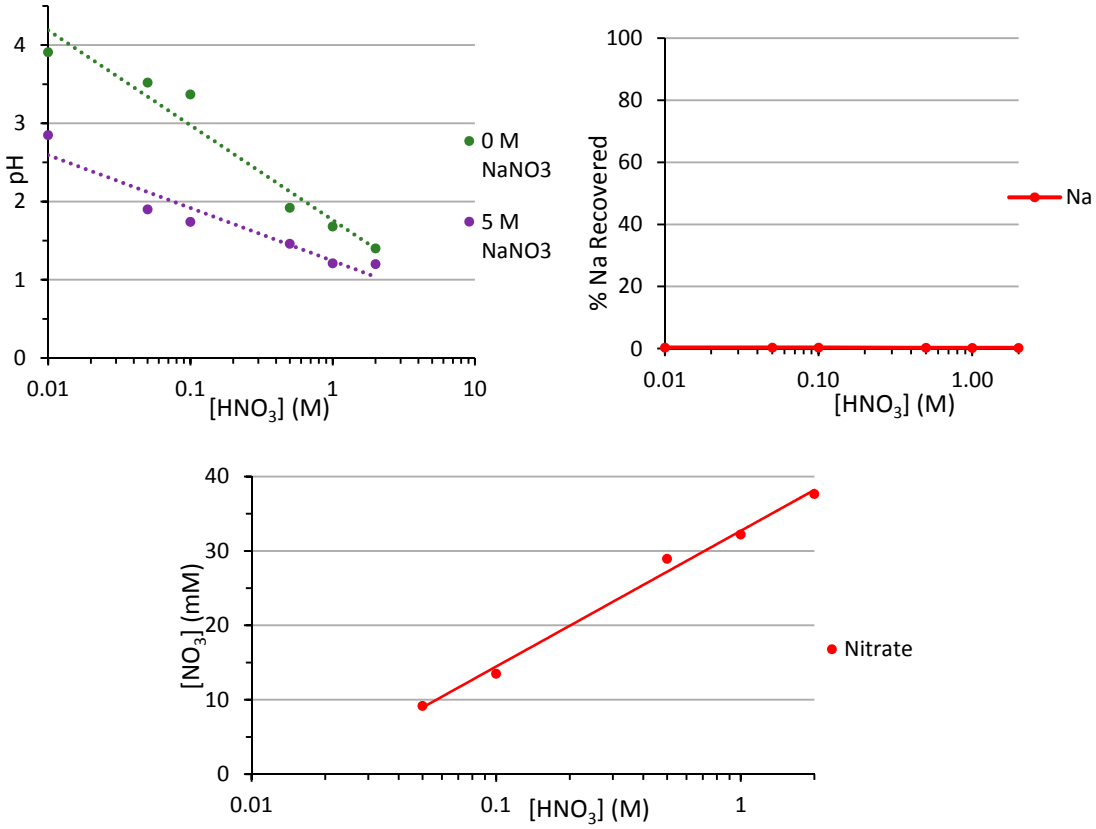

Figure 5. (**Top left**): The pH of aqueous solutions following contact of IL (0.1 M) in toluene loaded with HNO_3 (0.01–2.00 M) from $NaNO_3$ (0 and 5 M); (**top right**): The extraction of Na with **IL** (0.1 M) from 5 M $NaNO_3$ and HNO_3 (0.01–2.00 M) solution; (**bottom**): Determination of the concentration of NO_3^- extracted by **IL** using ion-chromatography. Interpolation used to aid the eye only.

3.2.3. Characterization by Mass Spectrometry and La NMR Spectroscopy

Negative-ion ESI-MS of the **IL** organic phases (0.1 M) loaded with La, Nd, and Dy (0.05 M) were recorded and show ions that comprise the metal cation, ammonium cations and NO_3^- anions of the general formula $Ln(NO_3)_4(\mathbf{IL})_n^-$ (where n is 0–3). The most prominent ion observed is for $n = 2$ at m/z 1252, i.e., $Nd(NO_3)_4(\mathbf{IL})_2^-$ that is also consistent with a formula of $[(octyl)_3NMe]_2[Ln(NO_3)_5]$ for the compound in the organic phase. Each ion seen experimentally displays isotopic patterns that agree with those calculated (Figure 6, Figure S3) and a repeating unit of 430.42 mass units is seen in each spectrum correlating to loss of **IL**.

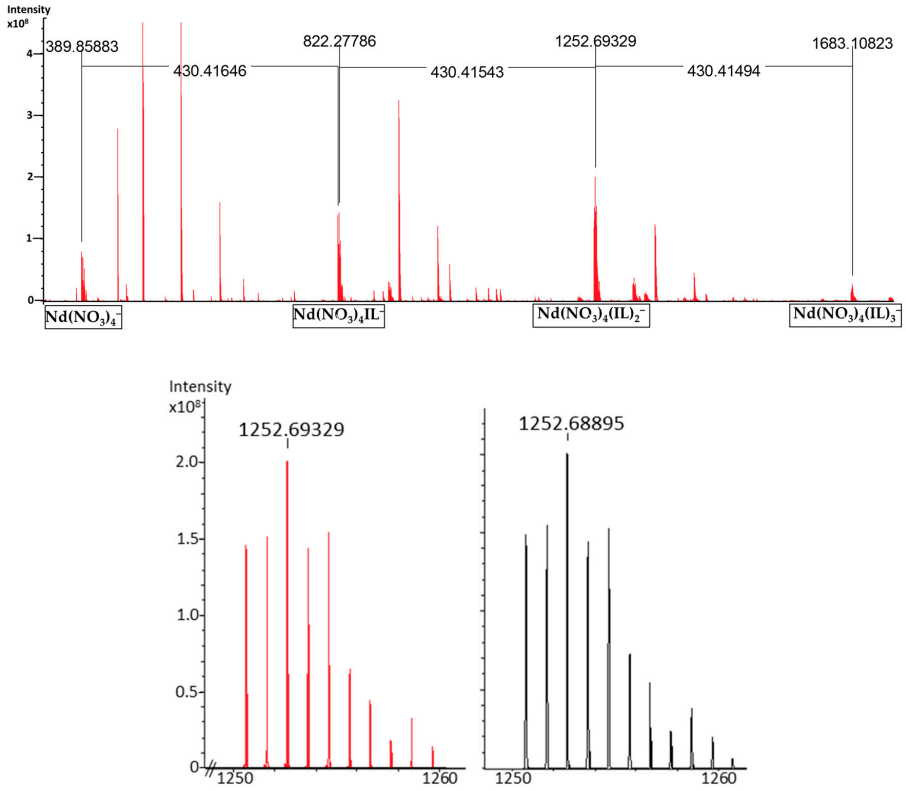

Figure 6. (**Top**): Negative-ion mode ESI-MS of the **IL** organic phase (0.1 M **IL**) post-contact with an Nd aqueous phase diluted with methanol showing ions of $Nd(NO_3)_4(IL)_n^-$ with m/z 391.8611 (n = 0, calc. 391.8596), 822.2779 (n = 1, calc. 822.2755), 1252.6933 (n = 2, calc. 1252.6890), and 1683.10823 (n = 3, calc. 1683.1024). (**Bottom**): Experimental negative-ion ESI-MS for n = 2 (red) compared with that calculated (black).

No ions that would suggest the presence of water in the organic phase are seen in the ESI-MS which corroborates the Karl-Fischer data above, although the dissociation of water from the supramolecular complex during ionization could occur [29]. To further probe the chemical environment of the species extracted into the hydrophobic phase, the ^{139}La NMR spectrum of the **IL** organic phase (0.05 M) after La extraction (0.05 M) was recorded and shows a single, broad resonance at −60 ppm when compared against $LaCl_3$ dissolved in water, i.e., $[La(H_2O)_6][Cl]_3$ (Figure 7). This chemical shift is consistent with the coordination of NO_3^- anions to La along with its dehydration [58], and the breadth of signal suggests that multiple, low symmetry nitrato complexes are present, as seen in the ESI-MS above; a variable temperature ^{139} La NMR study shows no significant change between +65 and +5 °C (Figure S4), mitigating against a dynamic process occurring.

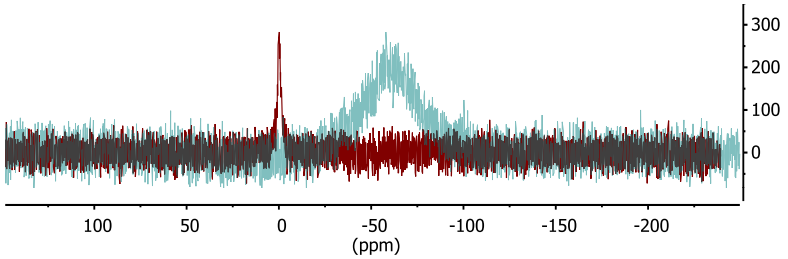

Figure 7. ^{139}La NMR spectra of the La standard, $LaCl_3$ (0.01 M, 0.0 ppm) in D_2O (red) and the **IL** organic phase (0.05 M) after contact with a 0.05 M aqueous La solution extraction **IL** (blue).

3.2.4. Structural Analysis by Computational Modelling

To understand further the interactions between **IL** and La compounds in the organic phase, a toluene solvent box of 60 Å^3 volume containing three **IL**s, three NO_3^- anions, three H_2O, and one La^{3+} cation was studied by classical MD techniques; these combinations are derived from the experimental information provided above (see Figure S5 for more details). Aggregation of all components in the solvent box is seen after 750 ps to form a partially hydrated La^{3+} cation with four NO_3^- anions within 5.1 Å of the La center, three H_2O molecules within 6.0 Å, and three nitrogen atoms from the encapsulating ammonium cations within 11 Å (Figure 8); all six NO_3^- are incorporated into the aggregate within 11 Å from the La^{3+} cation. It is clear that the formation of complexes in the organic phase is dynamic and that the nitrate anions and water molecules compete for interaction with the La^{3+} cation. This outcome is consistent with our previous studies on the ease of formation of La nitrato complexes in the aqueous phase, the breadth of resonance seen in the ^{139}La NMR spectrum, and that nitrate coordination is inferred by the presence of two peaks at 1435 and 1328 cm^{-1} in the IR spectrum of an **IL** organic phase loaded with La (Figure S6). Microhydration [59,60] of the La^{3+} cation, nitrate anions, and the ammonium cation may be important, as this may provide extra thermodynamic stability through hydrogen bonding, but quantum mechanical calculations are required to probe this further.

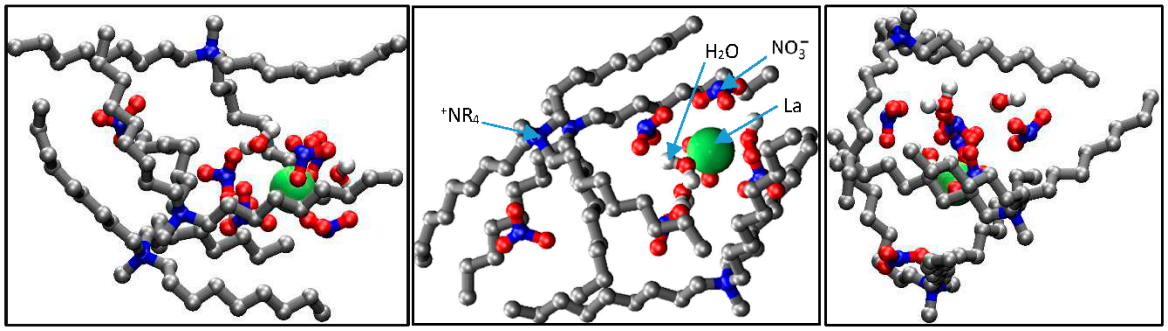

Figure 8. Three 'snapshot' images taken at 225 ps apart ((**left**) to (**right**)) from the classical MD simulations showing aggregation of water, nitrate, and ammonium cations around an La center within a 60 Å^3 box of toluene. For clarity, the toluene box is omitted, and H atoms are colored white, oxygen atoms red, nitrogen atoms blue, carbon atoms grey, and the La atom green.

The effectiveness of the encapsulation of the La cation and the attendant NO_3^- anions and water molecules by the lipophilic **IL** was probed by calculating the porosity of the aggregate using a Monte Carlo code. Here the La core (consisting of the La^{3+} cation, three water molecules, and six nitrate anions) is defined as the target, towards which a probe sphere is fired 10,000 times from random positions on the surface of a large sphere that encapsulates the aggregate; the number of probe spheres that successfully hit the core region (rather than be intercepted by the atoms on **IL**) is then recorded to give a percentage core exposure. In this way, the ability of **IL** to shield the La core can be quantified. From a random sample of 25 classical MD frames, the La core exposure was found to be 37 ± 3%; in contrast, targeting the La^{3+} cation exclusively reveals an exposure of 6.0 ± 1.3%. The simulations thus suggest that three **IL**s can be comfortably accommodated around a microhydrated La^{3+} cation.

4. Conclusions

This work has reinforced the efficacy of the [(*n*-octyl)$_3$NMe][NO_3] ionic liquid **IL** as a useful reagent for the recovery of REEs from mildly acidic, high nitrate salt, aqueous solutions. Extraction is fast and efficient, relatively selective for light REEs, and back-extraction may show additional selectivity if aqueous $NaNO_3$ is used. It can be concluded from the mode of action studies that the interactions between **IL** and REE nitrates are not (reverse) micellar; instead, ESI-MS, NMR, and computational

studies suggest that multiple NO_3^- anions are coordinated in the inner-sphere of a partially hydrated REE to form a series of anions $REE(NO_3)_n(H_2O)_x^-$ that are stabilized by electrostatic association with lipophilic NR_4^+ cations. Classical MD simulations for La suggest that the most prevalent species is $[(n\text{-octyl})_3NMe]_3[La(NO_3)_6(H_2O)_3]$ that incorporates a small number of water molecules in the hydrophobic phase through microhydration. We have shown previously that $La(NO_3)_4^-$ is unlikely to form in the aqueous phase [31], so it remains unclear in what form the REE is transported across the interface and whether complete dehydration of the metal occurs to facilitate transport across the phases. We are currently exploiting this mechanistic understanding to devise new, functionalized IL systems (Bif-ILs [2]) to engender stronger REE recovery from acidic feed streams and to be able to provide effective REE separation.

Supplementary Materials: The following are available online at http://www.mdpi.com/2075-4701/8/6/465/s1. Figure S1: Slope analysis; Figure S2: Back extraction (stripping) studies of La, Nd and Dy; Figure S3: La and Dy negative ion ESI-MS; Figure S4: Variable temperature ^{139}La NMR spectra; Figure S5: Computational outputs; Figure S6: Infrared spectra; Table S1: Distribution coefficients.

Author Contributions: J.B.L., B.T.N., and C.A.M. conceived and designed the experiments and simulations; J.P.H. and S.D. performed the experiments and simulations; J.B.L., C.A.M., B.T.N., J.P.H., and S.D. analyzed the data; J.P.H., C.A.M., and J.B.L. wrote the paper.

Funding: This research was funded by the Natural Environment Research Council, grant number NE/L002558/1.

Acknowledgments: We thank the School of Chemistry at the University of Edinburgh for funding and providing access to analytical facilities and to the Edinburgh Computer and Data Facility for access to high-performance computing facilities. This work was supported by a Natural Environment Research Council studentship to J.P.H. through the E3 DTP (grant number NE/L002558/1).

Conflicts of Interest: The authors declare no conflict of interest. The founding sponsors had no role in the design of the study; in the collection, analyses, or interpretation of data; in the writing of the manuscript; or in the decision to publish the results.

References

1. Rogers, R.D.; Seddon, K.R. Ionic Liquids—Solvents of the Future? *Science* **2003**, *302*, 792–793. [CrossRef] [PubMed]
2. Wang, K.; Adidharma, H.; Radosz, M.; Wan, P.; Xu, X.; Russell, C.K.; Tian, H.; Fan, M.; Yu, J. Recovery of rare earth elements with ionic liquids. *Green Chem.* **2017**, *19*, 4469–4493. [CrossRef]
3. Zhu, M.H.; Zhao, J.M.; Li, Y.B.; Mehio, N.; Qi, Y.R.; Liu, H.Z.; Dai, S. An ionic liquid-based synergistic extraction strategy for rare earths. *Green Chem.* **2015**, *17*, 2981–2993. [CrossRef]
4. Acharya, S.; Mishra, S. Studies on solvent extraction of La(III) using A336-NO_3 and modeling by statistical analysis and neural network. *Sep. Sci. Technol.* **2017**, *52*, 1660–1669. [CrossRef]
5. Rao, P.R.V.; Venkatesan, K.A.; Rout, A.; Srinivasan, T.G.; Nagarajan, K. Potential Applications of Room Temperature Ionic Liquids for Fission Products and Actinide Separation. *Sep. Sci. Technol.* **2012**, *47*, 204–222. [CrossRef]
6. Sun, X.Q.; Ji, Y.; Guo, L.; Chen, J.; Li, D.Q. A novel ammonium ionic liquid based extraction strategy for separating scandium from yttrium and lanthanides. *Sep. Purif. Technol.* **2011**, *81*, 25–30. [CrossRef]
7. Visser, A.E.; Rogers, R.D. Room-temperature ionic liquids: New solvents for f-element separations and associated solution chemistry. *J. Solid State Chem.* **2003**, *171*, 109–113. [CrossRef]
8. Cocalia, V.A.; Jensen, M.P.; Holbrey, J.D.; Spear, S.K.; Stepinski, D.C.; Rogers, R.D. Identical extraction behavior and coordination of trivalent or hexavalent *f*-element cations using ionic liquid and molecular solvents. *Dalton Trans.* **2005**, 1966–1971. [CrossRef] [PubMed]
9. Krishnamurthy, N.; Gupta, C.K. *Extractive Metallurgy of Rare Earths*; CRC Press: Boca Raton, FL, USA, 2004.
10. Liu, Y.H.; Chen, J.; Li, D.Q. Application and Perspective of Ionic Liquids on Rare Earths Green Separation. *Sep. Sci. Technol.* **2012**, *47*, 223–232. [CrossRef]
11. Jensen, M.P.; Neuefeind, J.; Beitz, J.V.; Skanthakumar, S.; Soderholm, L. Mechanisms of Metal Ion Transfer into Room-Temperature Ionic Liquids: The Role of Anion Exchange. *J. Am. Chem. Soc.* **2003**, *125*, 15466–15473. [CrossRef] [PubMed]

12. Okamura, H.; Aoyagi, N.; Shimojo, K.; Naganawa, H.; Imura, H. Role of Tf_2N-anions in the ionic liquid-water distribution of europium(iii) chelates. *RSC Adv.* **2017**, *7*, 7610–7618. [CrossRef]
13. Halpern, M. What Is Aliquat® 336 and Adogen® 464 HF? Let's Clear up the Confusion. Available online: http://phasetransfer.com/WhatisAliquat336andAdogen464.pdf (accessed on 1 June 2018).
14. Padhan, E.; Sarangi, K. Recovery of Nd and Pr from NdFeB magnet leachates with bi-functional ionic liquids based on Aliquat 336 and Cyanex 272. *Hydrometallurgy* **2017**, *167*, 134–140. [CrossRef]
15. Rout, A.; Venkatesan, K.A.; Srinivasan, T.G.; Rao, P.R.V. Ionic liquid extractants in molecular diluents: Extraction behavior of europium (III) in quarternary ammonium-based ionic liquids. *Sep. Purif. Technol.* **2012**, *95*, 26–31. [CrossRef]
16. Kumari, A.; Sinha, M.K.; Sahu, S.K.; Pandey, B.D. Solvent Extraction and Separation of Trivalent Lanthanides Using Cyphos IL 104, a Novel Phosphonium Ionic Liquid as Extractant. *Solvent Extr. Ion Exch.* **2016**, *34*, 469–484. [CrossRef]
17. Dupont, D.; Depuydt, D.; Binnemans, K. Overview of the Effect of Salts on Biphasic Ionic Liquid/Water Solvent Extraction Systems: Anion Exchange, Mutual Solubility, and Thermomorphic Properties. *J. Phys. Chem. B* **2015**, *119*, 6747–6757. [CrossRef] [PubMed]
18. Preston, J.S. The recovery of rare earth oxides from a phosphoric acid byproduct. Part 4. The preparation of magnet-grade neodymium oxide from the light rare earth fraction. *Hydrometallurgy* **1996**, *42*, 151–167. [CrossRef]
19. Morais, C.A.; Ciminelli, V.S.T. Selection of solvent extraction reagent for the separation of europium(III) and gadolinium(III). *Miner. Eng.* **2007**, *20*, 747–752. [CrossRef]
20. Larsson, K.; Binnemans, K. Separation of Rare Earths by Solvent Extraction with an Undiluted Nitrate Ionic Liquid. *J. Sustain. Metall.* **2017**, *3*, 73–78. [CrossRef]
21. Černá, M.; Bízek, V.; Šťastová, J.; Rod, V. Extraction of nitric acid with quaternary ammonium bases. *Chem. Eng. Sci.* **1993**, *48*, 99–103. [CrossRef]
22. Walker, I.M.; Weeden, D.H. Isotropic nuclear magnetic resonance shifts in ion-paired systems. Penta- and hexanitratolanthanate(III) complexes. *Inorg. Chem.* **1973**, *12*, 772–777. [CrossRef]
23. Bagreev, V.V.; Popov, S.O. NMR study of extracted compounds of trioctylalkylammonium with rare earth nitrates. *Polyhedron* **1985**, *4*, 929–932. [CrossRef]
24. Tao, G.H.; Huang, Y.; Boatz, J.A.; Shreeve, J.N.M. Energetic Ionic Liquids based on Lanthanide Nitrate Complex Anions. *Chem. Eur. J.* **2008**, *14*, 11167–11173. [CrossRef] [PubMed]
25. Roberts, R.J.; Ahern, J.C.; Patterson, H.H.; Leznoff, D.B. $Ce/Au(CN)_2^-$-Based Coordination Polymers Containing and Lacking Aurophilic Interactions. *Eur. J. Inorg. Chem.* **2016**, *2016*, 2082–2087. [CrossRef]
26. Chesman, A.S.R.; Turner, D.R.; Deacon, G.B.; Batten, S.R. Tetramethylammonium hexanitratoneodymiate(III). Structural variations of the $[Nd(NO_3)_6]^{3-}$ anion in a single crystal. *J. Coord. Chem.* **2007**, *60*, 2191–2196. [CrossRef]
27. Drew, M.G.B.; Hudson, M.J.; Iveson, P.B.; Russell, M.L.; Liljenzin, J.-O.; Sklberg, M.; Spjuth, L.; Madic, C. Theoretical and experimental studies of the protonated terpyridine cation. Ab initio quantum mechanics calculations, and crystal structures of two different ion pairs formed between protonated terpyridine cations and nitratolanthanate(III) anions. *J. Chem. Soc. Dalton Trans.* **1998**, 2973–2980. [CrossRef]
28. Liu, L.; Tian, G.; Rao, L. Effect of Solvation? Complexation of Neodymium(III) with Nitrate in an Ionic Liquid ($BumimTf_2N$) in Comparison with Water. *Solvent Extr. Ion Exch.* **2013**, *31*, 384–400. [CrossRef]
29. Ansari, S.A.; Liu, L.S.; Dau, P.D.; Gibson, J.K.; Rao, L.F. Unusual complexation of nitrate with lanthanides in a wet ionic liquid: A new approach for aqueous separation of trivalent *f*-elements using an ionic liquid as solvent. *RSC Adv.* **2014**, *4*, 37988–37991. [CrossRef]
30. Vander Hoogerstraete, T.; Binnemans, K. Highly efficient separation of rare earths from nickel and cobalt by solvent extraction with the ionic liquid trihexyl(tetradecyl)phosphonium nitrate: A process relevant to the recycling of rare earths from permanent magnets and nickel metal hydride batteries. *Green Chem.* **2014**, *16*, 1594–1606. [CrossRef]
31. Doidge, E.D.; Carson, I.; Love, J.B.; Morrison, C.A.; Tasker, P.A. The Influence of the Hofmeister Bias and the Stability and Speciation of Chloridolanthanates on Their Extraction from Chloride Media. *Solvent Extr. Ion Exch.* **2016**, *34*, 579–593. [CrossRef]

32. Carson, I.; MacRuary, K.J.; Doidge, E.D.; Ellis, R.J.; Grant, R.A.; Gordon, R.J.; Love, J.B.; Morrison, C.A.; Nichol, G.S.; Tasker, P.A.; et al. Anion Receptor Design: Exploiting Outer-Sphere Coordination Chemistry to Obtain High Selectivity for Chloridometalates over Chloride. *Inorg. Chem.* **2015**, *54*, 8685–8692. [CrossRef] [PubMed]
33. Wilson, A.M.; Bailey, P.J.; Tasker, P.A.; Turkington, J.R.; Grant, R.A.; Love, J.B. Solvent extraction: The coordination chemistry behind extractive metallurgy. *Chem. Soc. Rev.* **2014**, *43*, 123–134. [CrossRef] [PubMed]
34. Doidge, E.D.; Carson, I.; Tasker, P.A.; Ellis, R.J.; Morrison, C.A.; Love, J.B. A Simple Primary Amide for the Selective Recovery of Gold from Secondary Resources. *Angew. Chem. Int. Ed.* **2016**, *55*, 12436–12439. [CrossRef] [PubMed]
35. Jorgensen, W.L.; Maxwell, D.S.; Tirado-Rives, J. Development and Testing of the OPLS All Atom Force Field on Conformational Energetics and Properties of Organic Liquids. *J. Am. Chem. Soc.* **1996**, *118*, 11225–11236. [CrossRef]
36. Martinez, L.; Andrade, R.; Birgin, E.; Martinez, J.M. PACKMOL: A Package for Building Initial Configurations for Molecular Dynamics Simulations. *J. Comput. Chem.* **2009**, *30*, 2157–2164. [CrossRef] [PubMed]
37. Humphrey, W.; Dalke, A.; Schulten, K. VMD: Visual Molecular Dynamics. *J. Mol. Graph.* **1996**, *14*, 33–38. [CrossRef]
38. Frisch, M.J.; Trucks, G.W.; Schlegel, H.B.; Scuseria, G.E.; Robb, M.A.; Cheeseman, J.R.; Scalmani, G.; Barone, V.; Mennucci, B.; Petersson, G.A.; et al. *Gaussian 09*; Gaussian Inc.: Wallingford, UK, 2009.
39. Nosé, S. A Unified Formulation of the Constant Temperature Molecular Dynamics Methods. *J. Chem. Phys.* **1984**, *81*, 511–519. [CrossRef]
40. Hoover, W.G. Canonical Dynamics: Equilibrium Phase-Space Distributions. *Phys. Rev. A* **1985**, *31*, 1695–1697. [CrossRef]
41. Ab Rani, M.A.; Borduas, N.; Colquhoun, V.; Hanley, R.; Johnson, H.; Larger, S.; Lickiss, P.D.; Llopis-Mestre, V.; Luu, S.; Mogstad, M.; et al. The potential of methylsiloxanes as solvents for synthetic chemistry applications. *Green Chem.* **2014**, *16*, 1282–1296. [CrossRef]
42. Xie, F.; Zhang, T.A.; Dreisinger, D.; Doyle, F. A critical review on solvent extraction of rare earths from aqueous solutions. *Miner. Eng.* **2014**, *56*, 10–28. [CrossRef]
43. Torkaman, R.; Moosavian, M.A.; Torab-Mostaedi, M.; Safdari, J. Solvent extraction of samarium from aqueous nitrate solution by Cyanex301 and D2EHPA. *Hydrometallurgy* **2013**, *137*, 101–107. [CrossRef]
44. Quinn, J.E.; Soldenhoff, K.H.; Stevens, G.W.; Lengkeek, N.A. Solvent extraction of rare earth elements using phosphonic/phosphinic acid mixtures. *Hydrometallurgy* **2015**, *157*, 298–305. [CrossRef]
45. Ganji, S.; Shafaie, S.Z.; Goudarzi, N. Investigation of performances of solvents D2EHPA, Cyanex272, and their mixture system in separation of some rare earth elements from a Nitric Acid solution. *J. Min. Environ.* **2016**, *7*, 143–148. [CrossRef]
46. Jha, M.K.; Kumari, A.; Panda, R.; Kumar, J.R.; Yoo, K.; Lee, J.Y. Review on hydrometallurgical recovery of rare earth metals. *Hydrometallurgy* **2016**, *165*, 2–26. [CrossRef]
47. Xiong, Y.; Kuang, W.Q.; Zhao, J.M.; Liu, H.Z. Ionic liquid-based synergistic extraction of rare earths nitrates without diluent: Typical ion-association mechanism. *Sep. Purif. Technol.* **2017**, *179*, 349–356. [CrossRef]
48. Stojanovic, A.; Keppler, B.K. Ionic Liquids as Extracting Agents for Heavy Metals. *Sep. Purif. Technol.* **2012**, *47*, 189–203. [CrossRef]
49. Li, W.; Wang, X.L.; Zhang, H.; Meng, S.L.; Li, D.Q. Solvent extraction of lanthanides and yttrium from nitrate medium with CYANEX 925 in heptane. *J. Chem. Technol. Biot.* **2007**, *82*, 376–381. [CrossRef]
50. Banda, R.; Jeon, H.; Lee, M. Solvent extraction separation of Pr and Nd from chloride solution containing La using Cyanex 272 and its mixture with other extractants. *Separ. Purif. Technol.* **2012**, *98*, 481–487. [CrossRef]
51. MacRuary, K.J.; Gordon, R.J.; Grant, R.A.; Woollam, S.; Ellis, R.J.; Tasker, P.A.; Love, J.B.; Morrison, C.A. On the Extraction of HCl and H_2PtCl_6 by Tributyl Phosphate: A Mode of Action Study. *Solvent Extr. Ion Exch.* **2017**, *35*, 531–548. [CrossRef]
52. Nave, S.; Modolo, G.; Madic, C.; Testard, F. Aggregation properties of *N*,*N*,*N*′,*N*′-tetraoctyl-3-oxapentanediamide (TODGA) in *n*-dodecane. *Solvent Extr. Ion Exch.* **2004**, *22*, 527–551. [CrossRef]
53. Antonio, M.R.; McAlister, D.R.; Horwitz, E.P. An europium(III) diglycolamide complex: Insights into the coordination chemistry of lanthanides in solvent extraction. *Dalton Trans.* **2015**, *44*, 515–521. [CrossRef] [PubMed]

54. Ellis, R.J. Acid-switched Eu(III) coordination inside reverse aggregates: Insights into a synergistic liquid-liquid extraction system. *Inorg. Chim. Acta* **2017**, *460*, 159–164. [CrossRef]
55. Ansari, S.A.; Pathak, P.N.; Husain, M.; Prasad, A.K.; Parmar, V.S.; Manchanda, V.K. Extraction of actinides using *N*,*N*,*N*′,*N*′-tetraoctyl diglycolamide (TODGA): A thermodynamic study. *Radiochim. Acta* **2006**, *94*, 307–312. [CrossRef]
56. Ellis, R.J.; Meridiano, Y.; Chiarizia, R.; Berthon, L.; Muller, J.; Couston, L.; Antonio, M.R. Periodic Behavior of Lanthanide Coordination within Reverse Micelles. *Chem. Eur. J.* **2013**, *19*, 2663–2675. [CrossRef] [PubMed]
57. Jacox, M.E. Vibrational and electronic energy levels of polyatomic transient molecules. Supplement B. *J. Phys. Chem. Ref. Data* **2003**, *32*, 1–441. [CrossRef]
58. Evans, D.F.; Missen, P.H. La-139 Nuclear Magnetic-Resonance Spectra of Lanthanum Complexes. *J. Chem. Soc. Dalton Trans.* **1982**, 1929–1932. [CrossRef]
59. Walton, J. Microhydration and the Enhanced Acidity of Free Radicals. *Molecules* **2018**, *23*, 423. [CrossRef] [PubMed]
60. Gutberlet, A.; Schwaab, G.; Birer, Ö.; Masia, M.; Kaczmarek, A.; Forbert, H.; Havenith, M.; Marx, D. Aggregation-Induced Dissociation of $HCl(H_2O)_4$ Below 1 K: The Smallest Droplet of Acid. *Science* **2009**, *324*, 1545–1548. [CrossRef] [PubMed]